SHIMADZU
Excellence in Science

Application Note

No. 80

Life Science

Visualization of Glutamate Decarboxylase Activity Localization in Germinated Legume Seeds with the iMScope™ QT

Soichiro Ikuta[1], Naho Shinohara[1], Kaoru Nakagawa, Takushi Yamamoto, Eiichiro Fukusaki[1, 2, 3] and Shuichi Shimma[1, 2, 3]

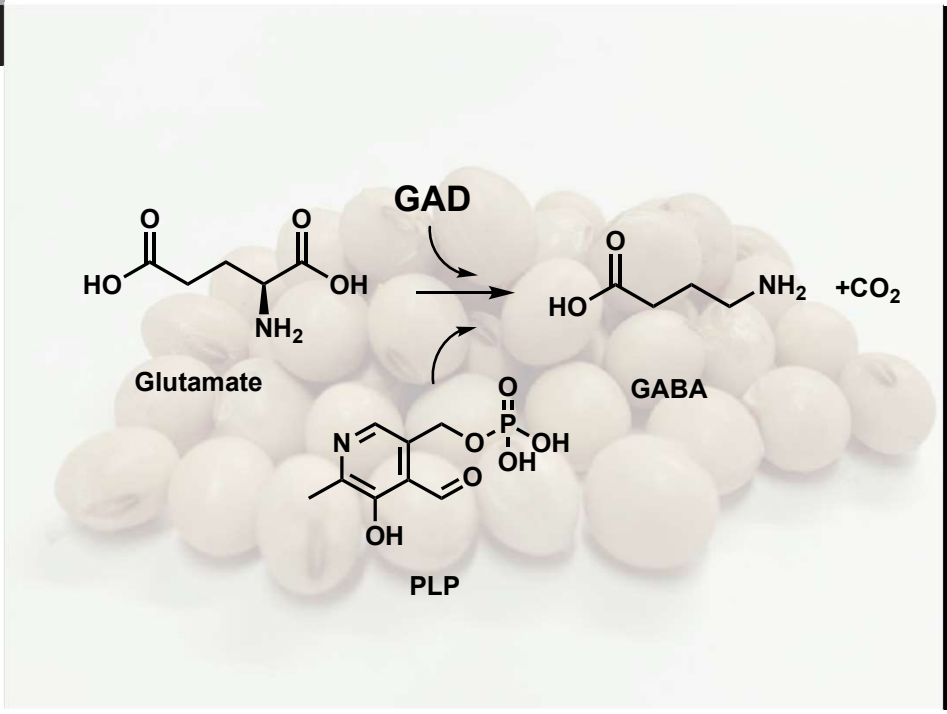

Life Science

■ Abstract

In vivo enzymatic reactions are normally detected by reacting the enzyme with a substrate, eliciting a color reaction with the resulting reaction products, and measuring absorbance or another indicator. Conventional detection methods require a primary reaction between the enzyme and substrate and a secondary reaction to produce color, while in more recent methods, these reactions are carried out on the tissue surface to visualize enzyme activity localization. This article describes a new enzyme histochemical method of detecting *in vivo* enzymatic reactions. using the high spatial resolution mass spectrometry imaging capabilities of the iMScope QT imaging mass microscope[1)].

1. Introduction

Determining *in vivo* enzyme activity localization is important for understanding physiological phenomena[2)]. Enzyme distribution is often studied using immunohistochemistry[3)] and *in situ* hybridization[4)], though these techniques only visualize the distribution of enzyme proteins or mRNA that code the amino acid sequence of the enzyme proteins, and cannot be used to visualize the distribution of actual enzyme activity. Enzyme histochemical methods, by contrast, can be used to visualize the distribution of enzyme activity on tissue sections[2)].

Enzyme histochemical methods have been used to visualize enzyme activity localization in plant samples since the 1960s[5)]. In one recent example, de Ávila *et al.* used enzyme histochemistry to visualize peroxidase (POD, EC 1.11.1.7) localization in the rind of *Vitis vinifera* L[6)]. Each enzyme is given an EC number, where EC is an abbreviation of Enzyme Commission and the first digit of the EC number groups enzymes into seven classes based on the general type of reaction catalyzed by the enzyme.

De Ávila *et al.* visualized POD by adding the substrate 3,3′-diaminobenzidine tetrahydrochloride (DAB) to POD in a tissue section and measuring the polymeric pigment generated from this substrate. Thus, conventional enzyme histochemistry can reveal the distribution of specific enzyme activities but requires a secondary reaction to produce color, which limits the enzymes that can be targeted by this technique.

We have established an approach that avoids color generation via secondary reactions by using mass spectrometry imaging (MS imaging) to detect and visualize the distribution of molecules produced in enzymatic reactions. Our research group has focused on small molecular weight metabolites and successfully used MS imaging to visualize cholinesterase (ChE)[7)] and choline acetyltransferase (ChAT)[8)] activity localization as well as dipeptidyl peptidase B activity localization in rice *koji*[9)].

[1]Department of Biotechnology, Graduate School of Engineering, Osaka University
[2]Osaka University Shimadzu Omics Innovation Research Laboratory, Osaka University
[3]Institute for Open and Transdisciplinary Research Initiatives, Osaka University

The enzyme targeted in this article, glutamate decarboxylase (GAD, EC 4.1.1.15), catalyzes the decarboxylation of L-glutamate to the amino acid γ-aminobutyric acid (GABA). Understanding the biosynthesis of GABA is important for the study of both food chemistry and plant physiology. In plants, GABA is involved in signal transduction, pH regulation, C/N ratio regulation, and responses to biotic and abiotic stress[10]. GABA is also reported to increase during germination in various plants such as soybean[11], rice[12], and barley[13], and is thought to play an important role in this seed germination. Foods that contain high levels of GABA are also attracting interest, with germinated legume seeds such as soybeans being marketed as GABA-rich foods. Understanding the distribution of GABA-synthesizing GAD in seeds during germination could therefore help to determine the role of GAD in plant seed germination, and this knowledge may be used to develop foods that are high in GABA. Although studying GAD activity in plants is important for these reasons, no methods for investigating tissue-specific GAD activity localization in plant seeds have been reported in the literature.

Therefore, the objective of this study was to use enzyme histochemistry with MS imaging to develop a method of visualizing GAD activity localization in germinated plant seeds. The samples used in developing this method were soybean (*Glycine max*) seeds and alfalfa (*Medicago sativa*) seeds, both of the legume family and often used as model plants in the food sciences. First, enzyme reaction conditions were optimized on plant tissue and used to investigate tissue-specific GAD activity localization in detail with the iMScope QT.

Fig. 1 The iMLayer™ Matrix Vapor Deposition System

Fig. 2 The iMScope™ QT Imaging Mass Microscope

Next, we investigated whether the method could also be applied to germinated alfalfa seeds, the tissues of which are difficult to separate due to their small size (around 3 mm).

2. Experiments

Soybean seeds procured from the Greenfield Project were placed on a bed of vermiculite, covered lightly with vermiculite, and incubated in the dark at 25 °C for 5 days to germinate. Alfalfa seeds were placed in a petri dish for 24 hours to germinate. Upon collection, germinated seeds were stored frozen at -80 °C.

Frozen sections were prepared by placing germinated soybean seeds and alfalfa seeds in a mold, embedding the seeds in 4% carboxymethyl cellulose solution (CMC solution), and freezing at -80 °C. The prepared sections were handled using Cryofilm (SECTION-LAB) adhesive film. Cryofilm with adhered tissue sections was immobilized on indium tin oxide (ITO) coated glass slides (Matsunami) with conductive double-sided tape (3M).

The GAD substrate solution used with both soybean and alfalfa seeds was a 70 mM phosphate buffer mixture (adjusted to pH 3.0, 5.8, and 8.0 to investigate optimal pH) with 2 mM EDTA and 0.2 mM PLP, adjusted to a final concentration of 50 mM Glu-d3. An airbrush (GSI Creos) was used to supply 50 µL of GAD substrate solution over the entire surface of each section. After supplying the substrate, tissue sections were reacted for between 0-30 minutes in a humidifying chamber heated at between 40, 50, and 60 °C.

The iMLayer™ matrix vapor deposition system (Fig. 1) was then used to coat the tissue sections with α-cyano-4-hydroxycinnamic acid (CHCA, Sigma-Aldrich) by vapor deposition using CHCA as the matrix.

MS imaging was performed using an MS imaging system consisting of an LCMS-9030 Q-TOF mass spectrometer connected to an iMScope QT atmospheric MALDI unit with built-in microscope (Fig. 2). Measurement conditions are shown in Table 1. All mass spectra were acquired in positive ion mode in the mass range *m/z* 95 to 155. Data were analyzed using IMAGEREVEAL™ MS imaging data analysis software (Fig. 3). Region of interest (ROI) analysis was performed on GAD activity images by using micrographs to identify specific areas and then creating ROIs of a specific size to encompass these areas. Bar graphs were prepared from mean intensity measurements in each ROI.

Significant differences between groups of three or more mean values were investigated with an ANOVA test with the Bonferroni test used for correction.

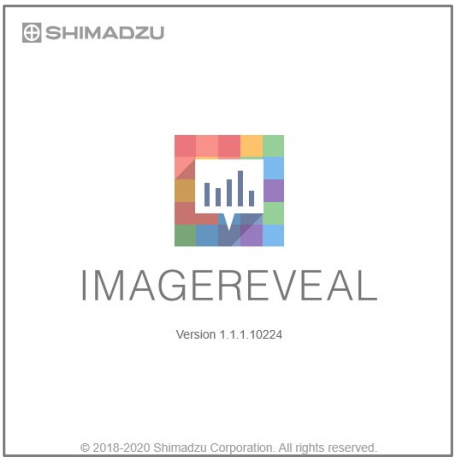

Fig. 3 IMAGEREVEAL™ MS Imaging Data Analysis Software

3. Results and Discussion

Confirming GABA is Synthesized by GAD

To confirm a GAD enzymatic reaction, we checked whether reaction products were synthesized from the substrate supplied to the soybean seed section. Glu-d3 substrate was supplied to the seed section with an airbrush, the seed section was incubated at 40 °C for 15 minutes, CHCA was applied to the seed section as a matrix coating, and MS imaging analysis was used to confirm the presence of the substrate and GABA-d3 reaction product on the soybean seed section. The resulting mean mass spectra detected Glu-d3 at *m/z* 151.08 and GABA-d3 at *m/z* 107.09 (Fig. 4).

To check whether the detected GABA was produced by soybean GAD in the tissue section, the same procedure was performed on sections deactivated in an autoclave. No GABA-d3 was detected in sections deactivated in an autoclave (data not shown). The above findings confirmed the presence of a GAD enzymatic reaction producing GABA-d3 from Glu-d3 in the soybean seed sections.

Table 1 iMScope QT Measurement Conditions

Measurement Mode:	**Positive**
Pitch (spatial resolution):	**25 µm**
***m/z* Range:**	**95-155**
Sample Voltage:	**3.50 kV**
Detector Voltage:	**2.50 kV**
Laser Irradiation Count:	**100**
Laser Repetition Frequency:	**1000 Hz**
Laser Irradiation Diameter Setting:	**2**
Laser Intensity	**77.6**

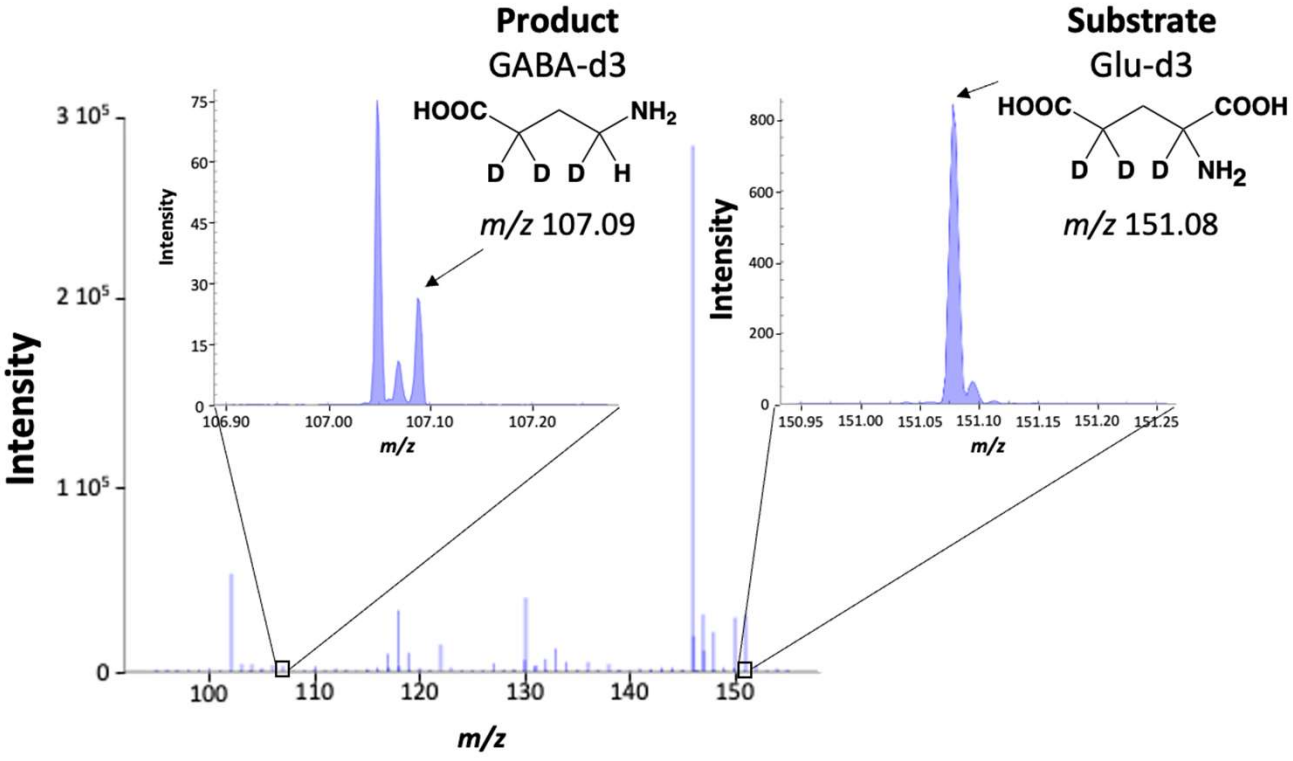

Fig. 4 Mass Spectrum of a Germinated Soybean Seed Section
The peak for the GABA-d3 reaction product (*m/z* 107.09) is larger than the peak for the Glu-d3 substrate (*m/z* 151.08).
Peak resolution is very good due to iMScope QT being a Q-TOF mass spectrometer.

Investigating GAD Reaction Conditions

The optimum substrate solution pH, enzyme reaction temperature, and enzyme reaction time conditions for visualization of GAD activity were investigated. GAD activity was significantly greater at substrate solutions of pH 5.8 and 8.0 than under strongly acidic conditions at pH 3.0 (Fig. 5A). Activity was greatest at pH 5.8, which was therefore chosen as the optimum substrate solution pH. Comparing enzyme reaction temperatures of 40 °C, 50 °C, and 60 °C showed that the higher the temperature, the greater the GAD activity, with a significant difference between 40 °C and 60 °C (Fig. 5B). We therefore chose 60 °C as the optimum reaction temperature. Upon supplying substrate solution, GABA-d3 increased linearly with incubation time between 0 and 5 minutes and plateaued after 5 minutes (data not shown). Based on these results, a reaction time of 3 minutes was chosen.

Visualizing GAD Activity in Germinated Seeds

The distribution of GAD activity in germinated seeds was visualized by performing GABA-d3 MS imaging analysis under the optimized reaction conditions described above. The results of this analysis are shown in Fig. 5C. The images in Fig. 5C show very little GABA-d3 was detected in the cotyledon and large amounts of GABA-d3 were detected in the hypocotyl. More specifically, most GABA-d3 was distributed near the tip of the hypocotyl away from the cotyledon. These findings suggest the majority of GAD activity was present in the hypocotyl of the germinated soybean seed and not in the cotyledon.

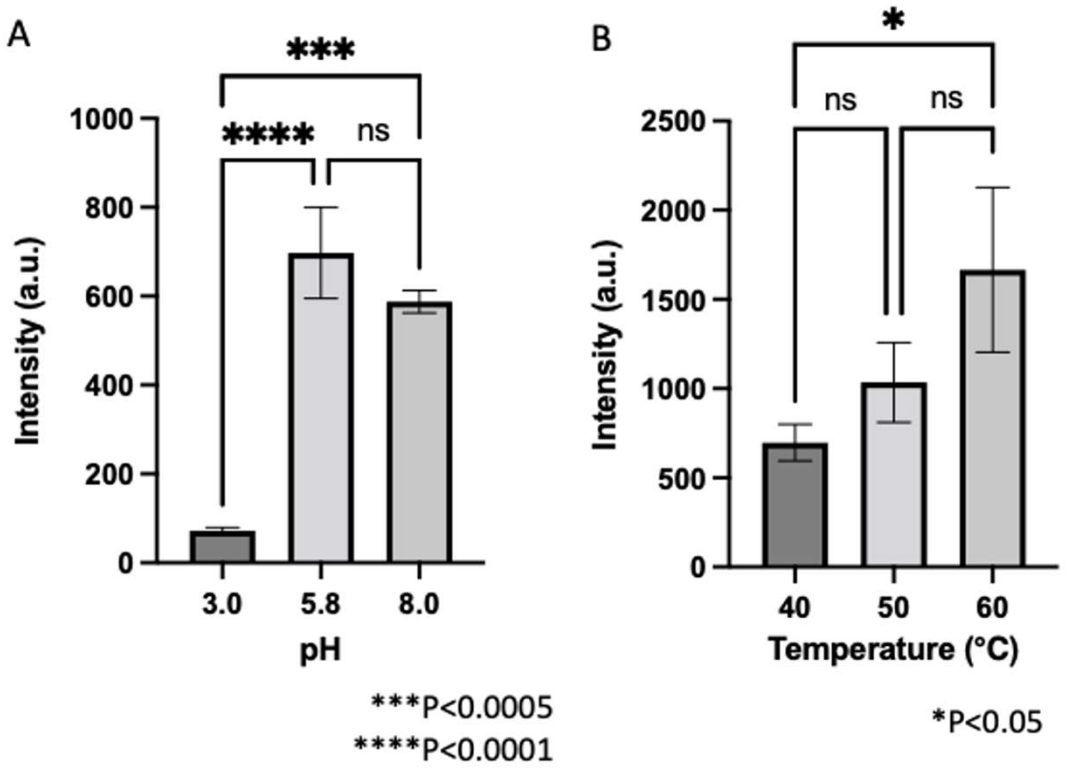

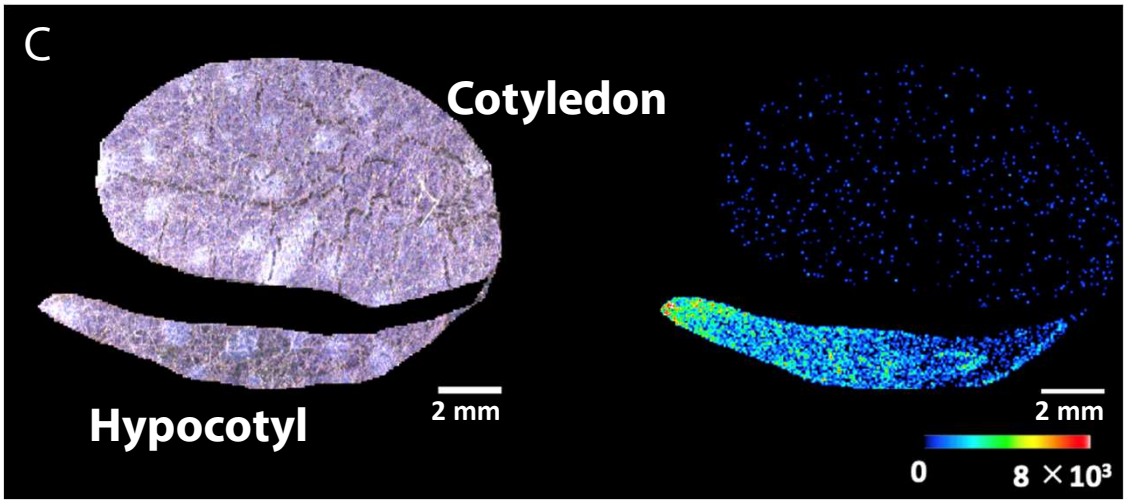

Fig. 5 Investigating Reaction Conditions and GAD Activity Distribution under Optimized Conditions on Soybean Seed Tissue Sections
(A) Effect of Substrate Solution pH on Activity, (B) Effect of Reaction Temperature on Activity, and (C) GABA-d3 Distribution at pH 5.8, 60 °C, and after a Reaction Time of 3 Minutes
MS imaging performed under optimum reaction conditions revealed GABA-d3 accumulation in the hypocotyl part of the germinated soybean section.

GAD Activity in the Hypocotyl of a Germinated Seed Under GAD Enzyme Reaction Conditions

The GABA-d3 MS imaging results for a whole germinated seed presented in Fig. 5C show the GABA-d3 distribution is influenced by histological structure, with higher GABA-d3 levels in the hypocotyl part of the seed. A high-resolution spatial analysis of the hypocotyl was attempted based on this finding (spatial resolution: 15 µm). The MS imaging results of this analysis are shown in Fig. 6A and reveal high levels of GABA-d3 distributed in the vascular system and root meristem of the hypocotyl, while the root parenchyma contains lower levels of GABA-d3 compared to the vascular system and root meristem.

Visualizing GAD Activity in Alfalfa Seeds

Alfalfa seeds are smaller than soybean seeds, being just 1-2 mm in size as seeds and increasing to 2-3 mm after water absorption and germination. Since it is difficult to separate the cotyledon and hypocotyl of alfalfa seeds, the alfalfa seed presents a good opportunity to demonstrate the utility of MS imaging. MS imaging of GABA-d3 was performed on germinated alfalfa seeds as for soybean seeds. The results of this analysis are shown in Fig. 6B. The MS images of GABA-d3 show a similar distribution to soybean seeds, with more GABA-d3 distributed in the tip of the hypocotyl (root tip) compared to the cotyledon and root parenchyma.

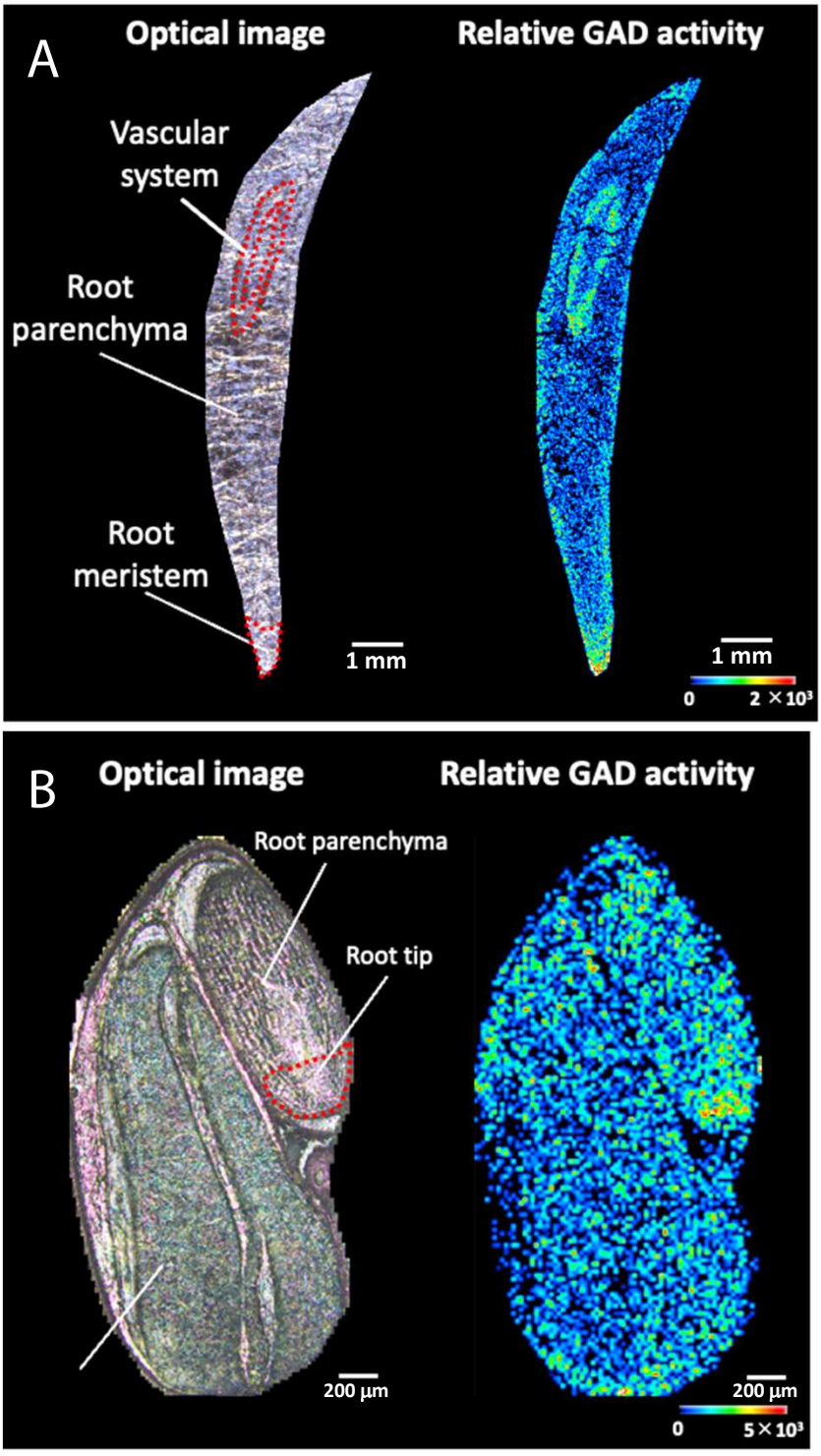

Fig. 6 (A) High Resolution Imaging of a Soybean Seed Hypocotyl and (B) MS Imaging of an Alfalfa Seed
MS imaging shows a higher ion intensity at the root tip in soybean and alfalfa seeds. The images indicate that GAD activity is greater in regions with active cell division.

4. Discussion

This study compared GAD activity under different reaction conditions by varying the substrate solution pH, enzyme reaction temperature, and enzyme reaction time. Previous studies featuring other plant species such as cowpea[14], potato[15], and germinated rice[16] have noted a pH of between 5.8 and 6.0 as optimum for GAD activity. A pH of 5.8 was also used in a study that measured GAD activity in soybeans[17], thereby supporting the substrate solution pH used to verify MS imaging in this study. The optimum temperature for GAD activity seems to differ depending on plant species, with 40 °C reported as the optimum temperature in faba bean[18] and potato[15] and 60 °C reported as the optimum temperature in germinated rice[16] and squash[19]. This study detected the highest GAD activity in germinated soybean seeds at 60 °C, suggesting that 60 °C is the optimum temperature for GAD activity in soybean. Regarding enzyme reaction times, as long as a sufficient amount of substrate remains available to GAD, the enzyme reaction rate is constant and reaction products increase linearly with reaction time. This study uses a relative GAD activity distribution based on the GABA-d3 intensity detected at a reaction time of 3 minutes, which is within the window of constant enzyme reaction rate conditions.

A previous report noted 2.81 times the GAD activity in soybean seeds after 40 hours of germination compared to ungerminated seeds[20], and GAD is known to become activated from an early point in soybean seed germination. The results of the present study are consistent with these past findings. GAD gene expression in soybean seeds is also reported to increase for up to 5 days after germination[21], and increased expression of the GAD gene may have caused an increase in enzyme activity in this study.

The GABA-d3 distribution detected in this study showed that increased GAD activity during germination is caused by increased GAD activity in the hypocotyl. In soybean seeds, the cotyledon is mainly responsible for storing and supplying nutrients and is not particularly active in terms of GABA biosynthesis during early germination. A previous study that separated the cotyledon and hypocotyl of soybean seeds[17] also showed greater GAD activity in the hypocotyl than in the cotyledon, which is consistent with the results of this study. The above findings indicate this study has successfully established a method of visualizing GAD activity localization in soybean seeds using MS imaging.

Furthermore, the greater GAD activity detected in the vascular system by high spatial resolution analysis is probably due to the vascular system being used to transport large molecular weight substances such as mRNA and proteins in addition to small molecules such as products of photosynthesis[22], hence the vascular system containing a large amount of GAD protein. Also, a previous study[23] that examined GAD activity, calcium (Ca) levels, and calmodulin (CaM) levels in a germinated soybean cotyledon and sections of root cut at 1 cm lengths reported increased GAD activity and Ca levels in the final 1 cm tip of the germinated soybean root compared to the cotyledon and other mature tissue. The same study also detected greater amounts of CaM in the final 1 cm root tip compared to other root pieces. Considering these findings, the higher GAD activity detected in the root tip meristem in the present study may be due to soybean GAD being a calcium/calmodulin-dependent (Ca^{2+}/CaM-dependent) enzyme[24].

This study also represents the first successful use of MS imaging to visualize GAD activity localization in germinated alfalfa seeds. As for soybean seeds, the higher GAD activity detected in the root tip of alfalfa seeds is probably due to the root tip being a region of active cell division.

5. Conclusion

This article describes the first successful visualization of GAD activity localization in soybean seeds by enzyme histochemistry with MS imaging. This method also showed how GAD activity is distributed over different parts of the seed, information that could not be determined by previous methods. Separating the different tissues of alfalfa seeds is difficult, but this method was able to visualize localized differences in GAD activity in different parts of the alfalfa seed, demonstrating the versatility of this method. This method can also be used to investigate GAD activity localization in plant seeds other than legume seeds. Plant species other than soybeans, such as germinated brown rice and germinated barley, are also marketed as GABA-rich foods, and this research could lead to a better understanding of the role of GAD in the germination of these seeds. Ultimately, this method could help in developing foods with higher levels of GABA.

GAD that is actively involved in GABA biosynthesis is also thought to be involved in the salt stress response of plants. Various plant species are reported to increase GAD activity and GAD gene expression during germination in response to salt stress.

For example, increased GAD gene expression has been connected to salt stress in soybean seeds[25], and the GABA metabolic pathway that includes GAD is thought to be involved in combined hypoxic and salt stress conditions in faba beans[26,27]. The method demonstrated here can show GAD activity localization in germinating seeds under salt stress, which could reveal the histological role of GAD in salt stress tolerance. Salt damage to crops due to excessive irrigation and other factors is a major global problem that affects seed germination[28]. Our method could also be of value to agricultural production, as understanding the role of GAD in salt stress tolerance during germination could lead to the creation of salt-tolerant plant varieties. Furthermore, because GABA biosynthesis is affected by regulation of GAD activity in response to stress during germination, this method could be applied in the field of food production to develop GABA-rich foods.

MS imaging is also a powerful tool for visualizing endogenous metabolites and exogenous compounds. MS imaging could be used to simultaneously visualize and compare the localization of endogenous metabolites, exogenous compounds, and enzyme activity. For example, bananas are reported to increase in GABA content during ripening after harvest[29], and bananas are attracting interest as a GABA-rich food in addition to germinated soybean, germinated barley, and germinated brown rice. GAD gene expression is also reported to increase during this ripening process[30]. However, no studies have examined GAD activity localization and how GAD activity varies during the ripening process in fruit. MS imaging could be used to simultaneously visualize the distribution of endogenous GABA and GAD activity localization during the fruit ripening process, and by comparing these data reveal the causal relationships of GABA and GAD activity in fruit. Such findings could contribute to the creation of GABA-rich fruit varieties.

Comparing the distribution of exogenous plant regulators and enzyme activity localization could indirectly reveal how plant regulators affect enzyme activity in plants. Such findings could be used to understand the mechanisms of action of known plant regulators and be useful in developing novel regulators.

Although this study focused on the visualization of GAD enzyme activity, our research group has also shown this method to be effective for the visualization of ChE and ChAT activity, as mentioned above. While it is beyond the scope of this article to discuss plant enzymes more broadly, we believe this simple technique for mapping enzyme metabolites by supplying reaction substrates to tissue surfaces can be used to effectively visualize the activity of many different plant enzymes.

< References >

1) Ikuta S at al Shinohara N, Fukusaki E, Shimma S. Mass spectrometry imaging enables visualization of the localization of glutamate decarboxylase activity in germinating legume seeds. J. Bioeng. Biosci., 134, 356-361 (2022).
2) Gomori, G. Microtechnical demonstration of phosphatase in tissue sections. Proceedings of the Society for Experimental Biology and Medicine 42, 23 (1939)
3) Walker, R. P., Chen, Z. H., Johnson, K. E., Famiani, F., Tecsi, L., and Leegood, R. C.: Using immunohistochemistry to study plant metabolism: The examples of its use in the localization of amino acids in plant tissues, and of phosphoenolpyruvate carboxykinase and its possible role in pH regulation, J. Exp. Bot., 52, 565–576 (2001).
4) Jiang, J.: Fluorescence in situ hybridization in plants: Recent developments and future applications, Chromosome Res., 3, 153–165 (2019).
5) Läuchli, A.: Cryostat technique for fresh plant tissues and its application in enzyme histochemistry, Planta, 70, 13–25 (1966).
6) Molero, M. E., Alarcón, M. V., Uriarte, D., Mancha, L. A., Moreno, D., and Francisco-Morcillo, J.: Histochemical and immunohistochemical analysis of enzymes involved in phenolic metabolism during berry development in *Vitis vinifera* L., Protoplasma, 256, 25–38 (2019).
7) Takeo, E., Fukusaki, E., and Shimma, S.: Mass spectrometric enzyme histochemistry method developed for visualizing *in situ* cholinesterase activity in *Mus musculus* and *Drosophila melanogaster,* Anal. Chem., 92, 12379–12386 (2020).
8) Takeo, E., Sugiura, Y., Ohnishi, Y., Kishima, H., Fukusaki,E., and Shimma, S.: Mass Spectrometric enzyme histochemistry for choline acetyltransferase reveals *de novo* acetylcholine synthesis in rodent brain and spinal cord*, ACS Chen. Neurosci.*, 12**,** 2079–2087 (2021).
9) A.P. Wisman, M. Minami, Y. Tamada, S. Hirohata, K. Gomi, E. Fukusa ki, S.Shimma Visualization of dipeptidyl peptidase B enzymatic reaction in rice koji using mass spectrometry imaging J. Biosci. Bioeng., 134 (2022), pp. 133-137
10) Li, L., Dou, N., Zhang, H., and Wu, C.: The versatile GABA in plants, Plant Signal Behav., 16, e1862565 (2021).
11) Matsuyama, A., Yoshimura, K., Shimizu, C., Murano, Y., Takeuchi, H., and Ishimoto, M.: Characterization of glutamate decarboxylase mediating gamma-amino butyric acid increase in the early germination stage of soybean (*Glycine max* [L.] Merr), J. Biosci. Bioeng., 107, 538–543 (2009).
12) Zhao, G., Xie, M., Wang, Y., and Li J.: Molecular mechanisms underlying γ-aminobutyric acid (GABA) accumulation in giant embryo rice seeds, J. Agric. Food Chem., 65 4883–4889 (2017**).**
13) AL-Quraan N., AL-Ajlouni Z., and Obedat D.: The GABA shunt pathway in germinating seeds of wheat (*Triticum aestivum* L.) and barley (*Hordeum vulgare* L.) under salt stress, Seed Sci Res., 29, 250–260 (2019).
14) Brandon, S. Johnson, Narendra, K. Singh, Joe, H. Cherry, and Robert, D. Locy.: Purification and characterization of glutamate decarboxylase from cowpea, Phytochemistry, 46, 39–44 (1997).
15) Sstyanarayan, V. and Nair, P. M.: Purification and characterization of glutamate decarboxylase from Solanum tuberosum, Eur. J. Biochem., 150, 53–60 (1985).
16) Pramai, P., Thanasukarn, P., Thongsook, T., Jannoey, P., Chen, F., and Jiamyangyuen, S.: Glutamate decarboxylase (GAD)extracted from germinated rice: Enzymatic properties and its application in Soymilk, J. Nutr. Sci. Vitaminol., 65 166–170 (2019).
17) Guo, Y., Yang, R., Chen, H., Song, Y., and Gu, Z.: Accumulation of γ-aminobutyric acid in germinated soybean (*Glycine max* L.) in relation to glutamate decarboxylase and diamine oxidase activity induced by additives under hypoxia, Eur. Food Res. Technol., 234, 679–687 (2012).
18) Runqiang, Y., Yongqi, Y., Qianghui G., and Zhenxin G.: Purification, properties and cDNA cloning of glutamate decarboxylase in germinated faba bean (*Vicia faba* L.), Food Chem., 138, 1945–1951 (2013).
19) Matsumoto, T., Yamaura I., and Funatsu M.: Improved purification and spectroscopic properties of squash glutamate decarboxylase, Biosci. Biotechnol. Biochem., 60, 889–890 (1996).
20) Yang, R., Feng, L., Wang, S., Yu, N., and Gu, Z.: Accumulation of γ-aminobutyric acid in soybean by hypoxia germination and freeze-thawing incubation, J. Sci. Food Agric., 96, 2090–2096 (2016).
21) Luo, X., Wang, Y., Li, Q., Wang, D., Xing, C., Zhang, L., Xu, T., Fang, F., and Wang, F.: Accumulating mechanism of γ-aminobutyric acid in soybean (*Glycine max* L.) during germination, Int. J. Food Sci., 53, 106–111 (2018).
22) Lucas, W.J., Groover, A., Lichtenberger, R., Furuta, K., Yadav, S.R., Helariutta, Y., He, X. Q., Fukuda, H., Kang, J., Brady, S. M., and other 6 authors**:** The plant vascular system: Evolution, development and functions, J. Integr. Plant Biol., 55, 294–388 (2013).
23) Oh, S., and Choi, W.: Changes in the levels of γ-aminobutyric acid and glutamate decarboxylase in developing soybean seedlings, J. Plant Res., 114, 309–313 (2001).
24) Snedden, W. A., Arazi, T., Fromm, H., and Shelp, B. J.: Calcium/calmodulin activation of soybean glutamate decarboxylase. Plant Physiol., 108, 543–549 (1995).
25) Yin, Y., Yang, R., Guo, Q., and Gu, Z.: NaCl stress and supplemental $CaCl_2$ regulating GABA metabolism pathways in germinating soybean, Eur. Food Res. Technol., 238, 781-788 (2014).
26) Yin, Y., Cheng, C., and Fang, W.: Effects of the inhibitor of glutamate decarboxylase on the development and GABA accumulation in germinating fava beans under hypoxia-NaCl stress. RSC Advances, 8, 20456-20461 (2018).
27) Yang, R., Wang, S., Yin, Y., and Gu, Z.: Hypoxia treatment on germinating faba bean (*Vicia faba* L.) seeds enhances GABA-related protection against salt stress. Chil. J. Agric. Res., 75, 184–191 (2015).
28) Tester, M. and Davenport, R.: Na+ tolerance and Na+ transport in higher plants. Ann. Bot., 91, 503–527 (2003).
29) Parijadi R., Yamamoto K., Ikram M., Dwivany F., Wikantika K, Putri S, Fukusaki E.: Metabolome Analysis of Banana (*Musa acuminata*) Treated With Chitosan Coating and Low Temperature Reveals Different Mechanisms Modulating Delayed Ripening. Front. Sustain. Food Syst., 6, (2022).
30) Hu, W., Liu, J., Yang, X., Zhang, J., Jia, C., Li, M., Xu, B., and Jin, Z.: Identification of a Gene Encoding Glutamate Decarboxylase Involved in the Postharvest Fruit Ripening Process in Banana. *HortScience horts*, *49*, 1056-1060 (2014)

First Edition: Feb. 2023

SHIMADZU

Shimadzu Corporation

www.shimadzu.com/an/

› Please fill out the survey

Related Products Some products may be updated to newer models.

› iMScope QT
Imaging Mass Microscope

Related Solutions

› Metabolomics

› Price Inquiry

› Product Inquiry

› Technical Service / Support Inquiry

› Other Inquiry